

Article

A New Kinematic Synthesis Model of Spatial Linkages for Designing Motion and Identifying the Actual Dimensions of a Double Ball Bar Test Based on the Data Measured

Zuping Liao, Shouchen Tang and Delun Wang *

School of Mechanical Engineering, Dalian University of Technology, Dalian 116081, China;
liao-zuping@mail.dlut.edu.cn (Z.L.)

* Correspondence: dlunwang@dlut.edu.cn

Abstract: This paper presents the new synthesis models of spatial linkages for designing measurement motion functions and ranges and identifying the actual dimension parameters. The spatial five-bar linkage is first introduced for the kinematic model of a double ball bar test of a two-axis rotary table. To design the ideal measurement motion and motion range of the double ball bar test, a novel saddle synthesis model of a spatial four-bar linkage RRSS is readily presented. Based on the output data measured from the double ball bar test, a new saddle synthesis model of a spatial five-bar linkage RRSPS is logically proposed for identifying their actual dimensions. Finally, three test cases and their results indicate that the new synthesis models presented in the paper can conveniently and efficiently calculate the measurement motion function and range and accurately identify the actual dimensions of the double ball bar test, which provides a suitable mathematical model for improving the accuracy of the double ball bar tests of a two-axis rotary table of machine tools.

Keywords: spatial linkage; kinematic synthesis; identification; double ball bar; two-axis rotary table; mechanism



Citation: Liao, Z.; Tang, S.; Wang, D. A New Kinematic Synthesis Model of Spatial Linkages for Designing Motion and Identifying the Actual Dimensions of a Double Ball Bar Test Based on the Data Measured. *Machines* **2023**, *11*, 919. <https://doi.org/10.3390/machines11090919>

Academic Editors: Zoltán Virág, Florin Dumitru Popescu and Andrei Andras

Received: 22 August 2023
Revised: 14 September 2023
Accepted: 20 September 2023
Published: 21 September 2023



Copyright: © 2023 by the authors. Licensee MDPI, Basel, Switzerland. This article is an open access article distributed under the terms and conditions of the Creative Commons Attribution (CC BY) license (<https://creativecommons.org/licenses/by/4.0/>).

1. Introduction

The kinematic synthesis of mechanisms is a classical topic in the field of mechanism and machine theory, providing a theoretical foundation for machine design, particularly kinematic design. While there are many methods for kinematic analysis and synthesis of mechanisms in the literature [1,2], which support the applications of mechanism design, there are still many problems to be solved, in both theory and practice, in mechanical engineering. For instance, the synthesis of spatial linkages and the accuracy of actual mechanisms are ongoing challenges in the field.

Double ball bar (DBB) tests are widely used for the accuracy testing of machine tools [3,4]. According to the current standards [5,6] and references [7,8], DBB tests are typically used for circular tests of linear axes, where the moving ball rotates around the fixed ball on an assumed circle. For two-axis rotary tables, the motion trajectory is more complex, and cradle-type rotary tables have motion range restrictions, making it necessary to design the measurement motion function and ranges of the DBB test. The existing method [9,10] for designing the test trajectory involves defining the circular test path as the intersection of a test plane and the spherical work space, allowing for the calculation of the motion of both rotary axes.

The accuracy of the DBB test is crucial for ensuring the precision of the measurements obtained. This accuracy is influenced by several factors, including the trajectories of the DBB as well as the mounting and structural errors of the object being measured [11,12]. For a circular test, deviations in the measured data caused by mounting position errors can be corrected by circle fitting [13–15]. However, this approach is not applicable for complex spatial curves, and it is difficult to determine the structural errors of the machine tool.

From the kinematic viewpoint, a DBB test of a two-axis rotary table can be regarded as a spatial five-bar linkage SPS-RR with two DOFs: the SPS theoretical kinematic chain plus the R-R actual kinematic chain with geometrical errors and elastic deformations [16,17]. Generally, the pair P has displacement as the output of RR-SPS during the DBB tests, whose values vary and reveal the change in the geometrical error. But the output of the DBB test has a theoretical variation function as the installation positions, even though R-R are ideal kinematic pairs with non-errors. Fortunately, all of these are the kinematic topics of mechanisms. To improve the accuracy of DBB tests, it is necessary to plan the motion of the five-bar linkage RR-SPS and precisely identify its actual dimensions. This highlights the need for theoretical and experimental research into the kinematic design of DBB tests.

For the kinematic synthesis of a spatial five-bar linkage for DBB tests of a two-axis rotary table, it is the first topic for the spatial linkage to have two reasonable motions and suitable motion ranges, such as a crank with a rocker and the full work space. Secondly, the dimensions of the spatial linkage are closer to an actual one and as precise as possible, especially the mounting positions of the DBB, which are precisely identified. Therefore, the topics of the kinematic design for DBB tests of a two-axis rotary table are to synthesize a spatial five-bar linkage that has a crank, rocker, the full work space, and precise, actual dimensions during the DBB test in practice.

While there have been many approaches to designing different mechanisms for various applications in recent years, synthesizing a spatial five-bar linkage with these given conditions is a new topic. These approaches include Kinematic Sensitivity Analysis and Dimensional Synthesis [18], Exact Path Synthesis [19], Advanced Motion Synthesis [20], and Inverted Modeling [21,22]. Based on kinematic analysis and the synthesis of linkages for both spherical and spatial motion, this paper presents saddle point program models for the analysis and synthesis of spatial linkages, RRSPS and RRSS. These models are discussed in detail for both planning the motion function and identifying the actual parameters of a double ball bar test of a two-axis rotary table based on the data measured with machine tools.

2. The Spatial Five-Bar Linkage of Double Ball Bar Tests of a Two-Axis Rotary Table

The double ball bar instrument is used to measure the accuracy of a two-axis rotary table of a machine tool; two precision balls are mounted on the spindle and the worktable of the machine tool, respectively, and the distance between the two balls is sensed during the DBB test. For this study, the accuracy of the DBB test and the kinematic model of a spatial five-bar linkage for the DBB test of a two-axis rotary table have to be set up according to the application cases.

2.1. Double Ball Bar Test of a Two-Axis Rotary Table

The A and C two-axis rotary worktable is taken in this paper, shown in Figure 1a, and the double ball bar is shown in Figure 1b.

The spatial motion of the worktable can be expressed in the fixed coordinate system $\{O_f, X_f, Y_f, Z_f\}$ established on the machine tool frame, and each coordinate axis is along the corresponding machine tool linear axis direction. A moving coordinate system $\{O_m, x_m, y_m, z_m\}$, is set up on the worktable, and the axis z_m is defined along the worktable rotation axis direction. A point P of the worktable can be expressed as a point vector R_{Pf} in $\{O_f, X_f, Y_f, Z_f\}$:

$$R_{Pf} = R_{Omf} + [M_{AC}]r_{Pm} \quad (1)$$

where R_{Omf} is the position vector of O_m in $\{O_f, X_f, Y_f, Z_f\}$, r_{Pm} is the position vector of point P in $\{O_m, x_m, y_m, z_m\}$, and $[M_{AC}]$ is the transformation matrix of two coordinate systems and expressed as follows:

$$[M_{AC}] = \begin{bmatrix} 1 & 0 & 0 \\ 0 & \cos \theta_{1A} & -\sin \theta_{1A} \\ 0 & \sin \theta_{1A} & \cos \theta_{1A} \end{bmatrix} \cdot \begin{bmatrix} \cos \theta_{2C} & -\sin \theta_{2C} & 0 \\ \sin \theta_{2C} & \cos \theta_{2C} & 0 \\ 0 & 0 & 1 \end{bmatrix} \quad (2)$$

where θ_{1A} and θ_{2C} are the machine tool A-axis and C-axis rotation angles, respectively.

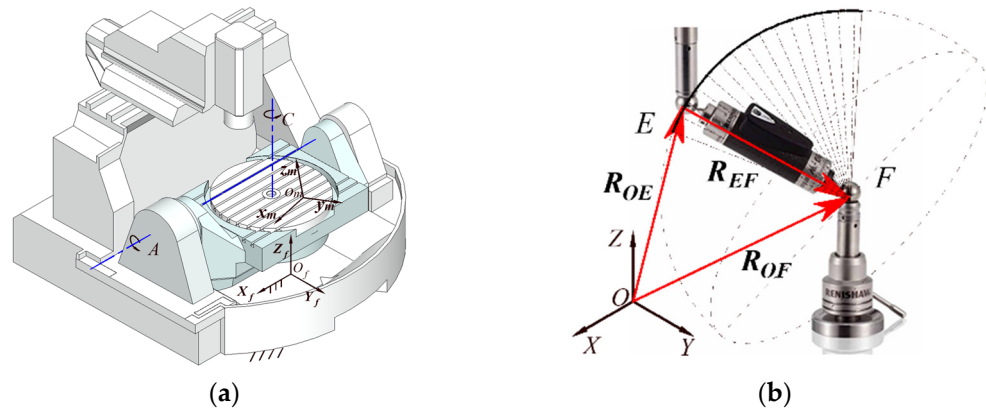


Figure 1. A and C two-axis rotary table and double ball bar: (a) A-C two-axis rotary table; (b) the double ball bar.

According to Equations (1) and (2), the orientation of the worktable can be located by adjusting the rotation angles θ_{1A} and θ_{2C} of the two rotary tables. In the practical use of the two rotary tables, the C-axis will rotate full-circle while the A-axis does a non-circle. The motion ranges of θ_{1A} and θ_{2C} are defined as follows:

$$\begin{cases} \theta_{1A} \in [\theta_{1Amin}, \theta_{1Amax}] \\ \theta_{2C} \in [0, 360) \end{cases} \quad (3)$$

In kinematic geometry, the motion of the two-axis rotary table can be viewed as the complex of two rotational motions, an open kinematic chain R-R. Two-axis A and C of the rotary table are independently driven by two motors, respectively.

The DBB is composed of two precision balls and a high-precision displacement sensor. The two precision balls are put on the magnetic ball seats that are fixed on the measured parts. Both precision balls can be viewed as two spherical kinematic pairs S. The high-precision displacement sensed is a prismatic pair P. Therefore, the kinematic chain of DBB is essentially viewed as SPS. The distance between the two precision balls, the relative displacement between points $E(x_E, y_E, z_E)$ and $F(x_F, y_F, z_F)$ of the DBB, is measured by the sensor, shown in Figure 1b. The vector connecting the two ball centers can be expressed by

$$\mathbf{R}_{EF} = \mathbf{R}_{OF} - \mathbf{R}_{OE} \quad (4)$$

where \mathbf{R}_{OE} and \mathbf{R}_{OF} are the position vectors of the two points E and F , respectively.

The length d of DBB is

$$d = |\mathbf{R}_{EF}| = \sqrt{(x_F - x_E)^2 + (y_F - y_E)^2 + (z_F - z_E)^2} \quad (5)$$

Usually, the length d of the DBB test of a two-axis rotary table is designated to be a constant for an ideal motion, but it is not so, even though it is an ideal motion in R-R.

2.2. The Mechanism Model for the DBB Test of a Two-Axis Rotary Table

In the field of kinematics, the DBB test for a two-axis rotary table is composed of two kinematic chains: RR and SPS. These chains are interconnected in a sequential manner, culminating in the formation of a closed-loop spatial five-bar linkage, referred to as RRSPS. Consequently, the kinematic geometry of the DBB test for a two-axis rotary table can be represented by an RRSPS spatial five-bar linkage, as shown in Figure 2.

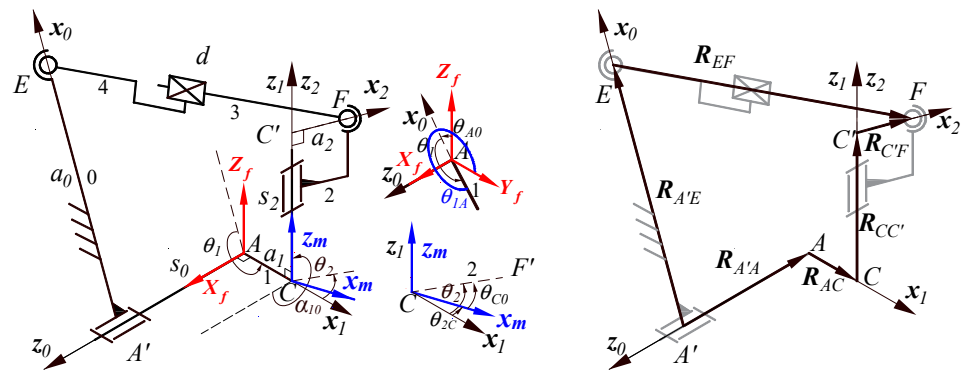


Figure 2. RRSPS linkage of DBB test of two-axis rotary table.

The spatial five-bar linkage RRSPS has five links, namely frame 0 and links 1, 2, 3, and 4, with the link lengths represented by $s_0, a_0, a_1, s_2, a_2,$ and α_{12} , as shown in Figure 2. This spatial linkage is driven by two input variables or motors that control the rotation angles θ_1 and θ_2 of links 1 and 2, respectively, wherein the output parameter ‘ d ’ is an independent variable representing the distance between the centers of the two balls. Pay attention to the variation of the output parameter ‘ d ’, which is confined to a small range in millimeters as dictated by the DBB instrument.

As per the Denavit–Hartenberg convention [23], the coordinate systems of three components of the spatial five-bar linkage are established. These include the fixed coordinate system $\{A', x_0, y_0, z_0\}$ for frame 0, the coordinate system $\{C, x_1, y_1, z_1\}$ for link 1, and the coordinate system $\{C', x_2, y_2, z_2\}$ for link 2. Two ball centers point $F (a_2 \cos\theta_{C0}, a_2 \sin\theta_{C0}, s_2)$ and $E (s_0, -a_0 \sin\theta_{A0}, a_0 \cos\theta_{A0})$ are, respectively, expressed in terms of the parameters of the linkage. A closed-loop vector equation is formulated to articulate the geometric relationships within the spatial five-bar linkage.

$$R_{EF} = R_{A'A} + R_{AC} + R_{CC'} + R_{C'F} - R_{A'E} \tag{6}$$

where, each vector denotes the position vector of the corresponding component in the fixed coordinate system, which can be expressed as follows:

$$\begin{cases} R_{Ef} = [X_{Ef} \ Y_{Ef} \ Z_{Ef}]^T = [s_0 \ -a_0 \sin \theta_{A0} \ a_0 \cos \theta_{A0}]^T \\ R_{Fm} = [x_{Fm} \ y_{Fm} \ z_{Fm}]^T = [a_2 \cos \theta_{C0} \ a_2 \sin \theta_{C0} \ s_2]^T \\ R_{AC} = [M_{10}] \cdot [a_1 \ 0 \ 0]^T \\ R_{CC'} = [M_{10}] \cdot [0 \ 0 \ s_2]^T \\ R_{C'F} = [M_{10}] \cdot [M_{21}] \cdot [a_2 \ 0 \ 0]^T \end{cases} \tag{7}$$

where the coordinate transformation matrix is

$$[M_{10}] = \begin{bmatrix} \cos \theta_1 & -\cos \alpha_{12} \sin \theta_1 & \sin \alpha_{12} \sin \theta_1 \\ \sin \theta_1 & \cos \alpha_{12} \cos \theta_1 & -\sin \alpha_{12} \cos \theta_1 \\ 0 & \sin \alpha_{12} & \cos \alpha_{12} \end{bmatrix} \quad [M_{21}] = \begin{bmatrix} \cos \theta_2 & -\sin \theta_2 & 0 \\ \sin \theta_2 & \cos \theta_2 & 0 \\ 0 & 0 & 1 \end{bmatrix}$$

By taking modulus on both sides of Equation (6) and substituting Equation (7) into (6), the basic displacement equation of the spatial five-bar RRSPS is obtained.

$$\begin{cases} d = \sqrt{(u^2 + v^2 + w^2)} \\ u = a_1 \cos \theta_1 + s_2 \sin \alpha_{12} \sin \theta_1 + a_2 \cos \theta_1 \cos \theta_2 - a_2 \cos \alpha_{12} \sin \theta_1 \sin \theta_2 - a_0 \\ v = a_1 \sin \theta_1 - s_2 \sin \alpha_{12} \cos \theta_1 + a_2 \sin \theta_1 \cos \theta_2 + a_2 \cos \alpha_{12} \cos \theta_1 \sin \theta_2 \\ w = -s_0 + s_2 \cos \alpha_{12} + a_2 \sin \alpha_{12} \sin \theta_2 \end{cases} \tag{8}$$

In Equation (8), there are a total of eleven parameters of the RR-SPS linkage, ($s_0, a_0, \theta_{A0}, s_2, a_2, \theta_{C0}, a_1, \alpha_{12}, \theta_1, \theta_2, d$), in which eight ones correspond to the constructure parameters

of the two-axis rotary table, one is the output parameter, while two are the input parameters. The parameters for the coordinates of the two balls' positions are $(s_0, a_0, \theta_{A0}, s_2, a_2, \theta_{C0})$, and the constructure parameters of the A-axis and C-axis are $(a_1$ and $\alpha_{12})$, the distance and angular between the A-axis and C-axis. The input angles θ_1 and θ_2 of the spatial five-bar linkage are the independent variables, and the output displacement d of the RR-SPS linkage can be solved by Equation (9). For the given parameters $(s_0, a_0, \theta_{A0}, s_2, a_2, \theta_{C0})$ of the coordinates of the two balls' positions, the length d of the spatial five-bar linkage RR-SPS varies or outputs different values.

The displacement d of the DBB test is measured for the actual motion of the A-axis and C-axis. In a theoretical case, both the A-axis and the C-axis have ideal motions or they rotate around their axis only, and the length of the DBB remains a theoretical function of the input angles θ_1 and θ_2 . In particular, d is a constant in two cases: (1) both the A-axis and the C-axis are the ideal orthogonal intersected axes, and two balls are specially located on the theoretical positions, and (2) the motion of the two input angles θ_1 and θ_2 has to be planned as a theoretical function relationship. Generally, case 2 is easy to be realized by designating the two input parameters θ_1 and θ_2 , which can be solved by the kinematics of a spatial four-bar RRSS linkage degenerated by RRSPS.

3. Motion Design of Spatial Four-Bar Linkage for the DBB Test of a Two-Axis Rotary Table

The DBB test of a two-axis rotary table is viewed as a spatial five-bar linkage RRSPS with two degrees of freedom, whose motions of two input parameters θ_1 and θ_2 must be designed for the DBB test, and the dimensions of the links must also be determined. In fact, the motion plan of the RRSPS is to determine the relationship between the two input parameters θ_1 and θ_2 . The design of the dimensions for the RRSPS involves determining the installation positions of both precision balls in order to measure the full workspace of the two rotary axes. Specifically, the A-axis has its own workspace with two extreme positions, while the C-axis can achieve a full rotation.

It is clear that designing both the motion and dimensions of the RRSPS involves obtaining two input motions that allow for variation in the output parameter d within a given range, while covering the full workspace of the two-axis rotary table during a DBB test. That is, a spatial four-bar linkage RRSS (crank-rocker) is synthesized, where link 2 is a crank with an input angle θ_2 , while link 1 is a rocker with an input angle θ_1 corresponding to its two extreme positions. The variation in displacement d during a DBB test remains zero in cases where there is an ideal motion for RR when both input angles θ_1 and θ_2 follow a theoretical function.

3.1. Motion Function Design for the DBB Test

A spatial five-bar linkage RRSPS accurately describes the kinematics of the DBB test for a two-axis rotary table during the measuring process. However, the motion function of the A-axis and C-axis must first be assigned, as the output length d of the DBB test varies with the rotation of the two axes. Specifically, the spatial five-bar linkage RRSPS of the DBB test for a two-axis rotary table can be simplified as a spatial four-bar RRSS linkage. In this case, the angles θ_1 and θ_2 have a theoretical function, and the output length d of the DBB test remains constant when the A and C axes have ideal motion.

A spatial four-bar linkage RRSS with one degree of freedom is shown in Figure 3, where frame 0 is converted into link 1 for a convenient angle relationship calculation.

This kinematic model is used to design the measurement motion of the two-axis rotary table or to determine the ideal motion function between the A and C axes. In practice, each axis is independently driven by a motor, but their rotation follows the function calculated by the spatial four-bar linkage RRSS.

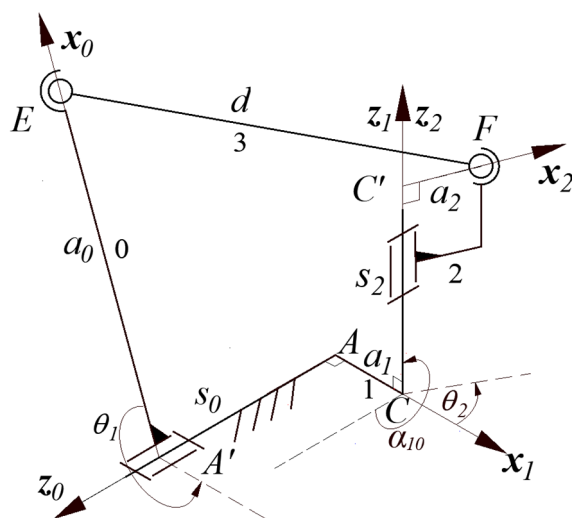


Figure 3. RRSS linkage of the DBB test of an ideal two-axis rotary table.

The spatial four-bar linkage RRSS also has eleven parameters ($s_0, a_0, \theta_{A0}, s_2, a_2, \theta_{C0}, a_1, \alpha_{12}, \theta_1, \theta_2, d$), which are the same as those of RRSPS, shown in Figure 3. The parameters of two balls' positions coordinates are ($s_0, a_0, \theta_{A0}, s_2, a_2, \theta_{C0}$), and the constructure parameters of the A-axis and C-axis are (a_1 and α_{12}). The length d of link 3, the distance between two balls, is a constant. The rotational angle θ_1 of link 1 is defined as the independent variable, or the input parameter, while the output angle θ_2 of link 2 is the dependent variable or a function of angle θ_1 . Based on Figure 3 and Equation (8), the motion relationship between the dependent variable θ_2 and the independent variable θ_1 can be derived as follows:

$$\begin{cases} A \sin \theta_1 + B \cos \theta_1 + C = 0 \\ A = 2a_0a_2 \cos \alpha_{12} \sin \theta_2 - 2a_0s_2 \sin \alpha_{12} \\ B = -2a_0a_2 \cos \theta_2 - 2a_0a_1 \\ C = a_0^2 + a_1^2 + a_2^2 + s_0^2 + s_2^2 - d^2 - 2s_0s_2 \cos \alpha_{12} - 2a_2s_0 \sin \alpha_{12} \sin \theta_2 + 2a_1a_2 \cos \theta_2 \end{cases} \quad (9)$$

On the other hand, θ_1 is expressed as the dependent variable while θ_2 is designated as the independent variable.

$$\begin{cases} L \sin \theta_2 + M \cos \theta_2 + N = 0 \\ L = 2a_0a_2 \cos \alpha_{12} \sin \theta_1 - 2a_2s_0 \sin \alpha_{12} \\ M = 2a_1a_2 - 2a_0a_2 \cos \theta_1 \\ N = a_0^2 + a_1^2 + a_2^2 + s_0^2 + s_2^2 - d^2 - 2a_0a_1 \cos \theta_1 - 2a_0s_2 \sin \alpha_{12} \sin \theta_1 - 2s_0s_2 \cos \alpha_{12} \end{cases} \quad (10)$$

Equations (9) and (10) reveal the relationship between the input parameter θ_1 and the output parameter θ_2 of the spatial four-bar linkage RRSS. The rotational angles θ_1 of link 1 and θ_2 of link 2 are expressed in the coordinate system of RRSS, which can be converted into the coordinate system of the machine tool, and the angle θ_{1A} of the A-axis and the orientation angle θ_{2C} of the C-axis of a two-axis rotary table can be expressed, respectively,

$$\begin{cases} \theta_{1A} = \theta_1 + \theta_{A0} + 90^\circ \\ \theta_{2C} = \theta_2 - \theta_{C0} \end{cases} \quad (11)$$

In Equation (11), θ_{A0} and θ_{C0} have the geometrical meanings of the installation initial angles of the spherical joints S_E and S_F in the coordinate system of the machine tool.

By substituting the calculation results of either Equations (9) or (10) into Equation (11), two motion relationship between the orientation angles θ_{1A} and θ_{2C} of the two-axis rotary table for the DBB test can be calculated. For a general RRSS linkage, the orientation angles θ_{1A} and θ_{2C} only belong to a part of the workspace of the two-axis rotary table. It is necessary to design both the reasonable installation parameters of the DBB and the

corresponding functions of θ_{1A} and θ_{2C} , that is to say, for the length of the DBB test to have a full work space, a crank, and a rocker.

3.2. Motion Range of the DBB Test of an Ideal Two-Axis Rotary Table

The RRSPS linkage of the DBB test for a two-axis rotary table, when in ideal motion, can be simplified to a spatial four-bar RRSS linkage, as shown in Figure 4. A spatial crank-rocker four-bar linkage needs to be synthesized, which has the motion range when link 2 rotates its angular θ_2 (0,360) and link 0 occupies its extreme positions, or θ_1 ($\theta_{1\min}$ and $\theta_{1\max}$). According to Section 3.1, the output parameter θ_1 and the input parameter θ_2 of the four-bar linkage RRSS correspond to their extreme values or locations. Based on the relationship between θ_1 and θ_2 , Equation (10) can be rewritten as

$$(M - N) \tan^2 \frac{\theta_2}{2} - 2L \tan \frac{\theta_2}{2} - (M + N) = 0$$

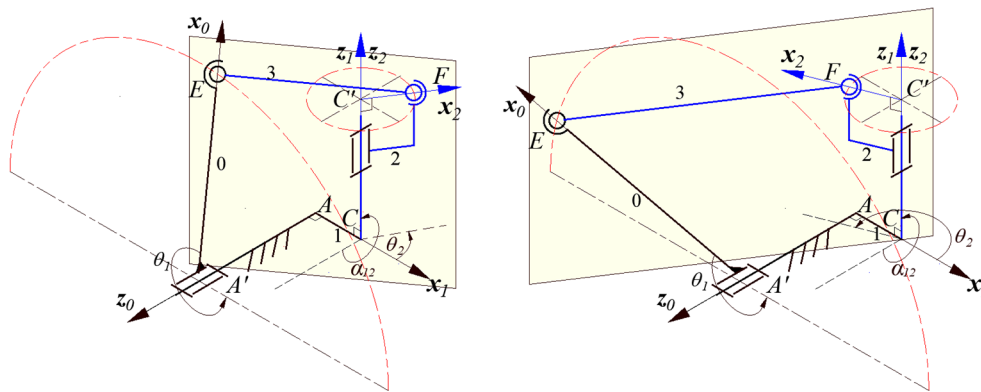


Figure 4. Extreme positions of the rocker of the spatial four-bar linkage RRSS.

The condition for the above equation to have a unique solution for the input parameter θ_2 is expressed as

$$L^2 + M^2 - N^2 = 0 \tag{12}$$

Additionally, when rocker 0 of the spatial four-bar linkage RRSS locates at the extreme position while crank 2 does at the dead point position, the instantaneous change rate (instantaneous velocity) of θ_1 relative to θ_2 is zero, expressed by

$$\frac{d\theta_1}{d\theta_2} = 0 \tag{13}$$

Taking the differential of both sides of Equation (10), and then substituting Equation (13) into the resulting differential equation, we can achieve the expression of θ_1 when rocker 0 is at the extreme position.

$$\theta_2 = \arctan \frac{s_0 \sin \alpha_{12} - a_0 \cos \alpha_{12} \sin \theta_1}{a_0 \cos \theta_1 - a_1} \tag{14}$$

Similar to the co-linearity condition of the crank and link in a planar four-bar linkage when the planar crank-rocker linkage is at the extreme position, the spatial position relationship between crank 2, link 3, and the rotation axis z_1 of the spatial four-bar linkage RRSS is discussed when rocker 0 is located at the extreme position. That is, three vectors, direction vector x_1 of crank 2, direction vector z_1 of its rotation axis, and vector R_{EF} of link 2, will be coplanar, as shown in Figure 4, and their inner product is zero:

$$(z_1, x_2, R_{EF}) = a_0 \cos \theta_1 \sin \theta_2 - a_1 \sin \theta_2 - s_0 \sin \alpha_{12} \cos \theta_2 + a_0 \cos \alpha_{12} \sin \theta_1 \cos \theta_2 = 0 \tag{15}$$

RRSS linkage finds out the two sphere centers, the moving sphere point $F(x_{Fm}, y_{Fm}, z_{Fm})$ of link 2 and the fixed sphere point $E(x_{Ef}, y_{Ef}, z_{Ef})$ of the frame link 0, respectively.

Based on the coordinate systems above, the moving point $F(x_{Fm}, y_{Fm}, z_{Fm})$ of link 2 traces a spatial trajectory $\Gamma_F: R_F(i), i = 1, \dots, n$ in the frame link 0, as link 1 and link 2 rotate $\theta_1^{(i)}, \theta_2^{(i)}$, which can be expressed as follows:

$$\begin{bmatrix} x_{Ff} \\ y_{Ff} \\ z_{Ff} \\ 1 \end{bmatrix} = [M_{10}] \cdot [M_{21}] \cdot \begin{bmatrix} x_{Fm} \\ y_{Fm} \\ z_{Fm} \\ 1 \end{bmatrix} \tag{17}$$

where

$$[M_{10}] = \begin{bmatrix} \cos \theta_1 & -\cos \alpha_{12} \sin \theta_1 & \sin \alpha_{12} \sin \theta_1 & -a_0 \\ \sin \theta_1 & \cos \alpha_{12} \cos \theta_1 & -\sin \alpha_{12} \cos \theta_1 & 0 \\ 0 & \sin \alpha_{12} & \cos \alpha_{12} & 0 \\ 0 & 0 & 0 & 1 \end{bmatrix} [M_{21}] = \begin{bmatrix} \cos \theta_2 & -\sin \theta_2 & 0 & 0 \\ \sin \theta_2 & \cos \theta_2 & 0 & 0 \\ 0 & 0 & 1 & 0 \\ 0 & 0 & 0 & 1 \end{bmatrix}$$

Hence, the kinematic synthesis of RRSS sets up the optimization model to locate the moving point $F(x_{Fm}, y_{Fm}, z_{Fm})$, whose trajectory Γ_F is the closest spherical curve.

We introduce the conception of the saddle spherical surface and its error in treatise [24], that is, for the given discrete point set $\{R_F^{(i)}\}$, a spherical surface adaptively determined by letting the maximum fitting error be minimum, whose spherical surface is the saddle spherical surface and the error is defined as the saddle spherical surface error. Based on the definition, we set up the mathematics model of a saddle spherical surface fitting as

$$\begin{cases} \Delta_{ss} = \min_x \max_{1 \leq i \leq n} \{ \Delta^{(i)}(x) \} \\ = \min_x \max_{1 \leq i \leq n} \left\{ \left| \sqrt{(x_{Ef} - x_{Ff}^{(i)})^2 + (y_{Ef} - y_{Ff}^{(i)})^2 + (z_{Ef} - z_{Ff}^{(i)})^2} - d \right| \right\} \\ s.t. g_j(x) \leq 0, j = 1, \dots \\ x = (x_{Ef}, y_{Ef}, z_{Ef}, d)^T \end{cases} \tag{18}$$

where the objective function $\{\Delta^{(i)}(x)\}$ is the normal fitting error of the discrete point set $\{R_F^{(i)}\}$ and a fitting spherical surface, the optimization variables $x = (x_{Ef}, y_{Ef}, z_{Ef}, d)$ are the saddle sphere center's coordinates (x_{Ef}, y_{Ef}, z_{Ef}) of link 0 and its diameter d , respectively; n is the number of discrete points $\{R_F^{(i)}\}$ and Δ_{ss} is the saddle spherical surface fitting error for $\{R_F^{(i)}\}$, which is called the first saddle program.

Obviously, one moving sphere point $F(x_{Fm}, y_{Fm}, z_{Fm})$ of link 2 is firstly chosen in link 2, which corresponds to a saddle sphere with its center's coordinates (x_{Ef}, y_{Ef}, z_{Ef}) and diameter d . For the moving link 2 with given discrete parameters $(x_{omf}^{(i)}, y_{omf}^{(i)}, z_{omf}^{(i)}, \theta_1^{(i)}, \theta_2^{(i)})$, there certainly exists a point $F(x_{Fm}, y_{Fm}, z_{Fm})$ whose trajectory corresponds to a saddle spherical surface error, which achieves a minimum value with respect to the other points in its neighborhood, which is called the saddle sphere point of link 2. On the other hand, the spatial RRSS linkage has to meet not only the kinematics but also non-geometrical inference, etc. We present the optimization mathematic model of a saddle synthesis of RRSS linkage for the DBB test as follows:

$$\begin{cases} \delta_{ss} = \min_x \Delta_{ss}(Z) \\ s.t. g_j(Z) \leq 0, j = 1, \dots \\ Z = (x_{Fm}, y_{Fm}, z_{Fm})^T \end{cases} \tag{19}$$

where $\Delta_{ss}(Z)$ is the objective function or the saddle spherical surface error for any point trajectory $\{R_F^{(i)}\}$, obtained by Equation (17), $Z = (x_{Fm}, y_{Fm}, z_{Fm})$ are the optimization variables.

δ_{ss} is the saddle sphere point error. It is called the second saddle program. The constraint equations are given as follows according to the DBB test device and process.

(1) The moving bounds of the spherical pair: the ball bar rotates around the sphere center, which must be constrained in the bounds of DBB construction:

$$\begin{cases} g_1(\mathbf{x}) = \arccos \frac{\mathbf{R}_{EF} \cdot (-\mathbf{x}_0)}{|\mathbf{R}_{EF}|} - \alpha_{EF} \leq 0 \\ g_2(\mathbf{x}) = \arccos \frac{\mathbf{R}_{EF} \cdot \mathbf{z}_2}{|\mathbf{R}_{EF}|} - \alpha_{EF} \leq 0 \end{cases} \quad (20)$$

(2) Interference conditions of the ball bar and the rotary table:

$$g_3(\mathbf{x}) = \{r_{LEF}(t_L) \cap r_S(t_S, \varphi_S)\} = \emptyset \quad (21)$$

where r_{LEF} is the vector function of the ball bar

$$r_{LEF}(t_L) = \mathbf{R}_E + t_L \cdot \frac{\mathbf{R}_{EF}}{|\mathbf{R}_{EF}|}, t_L \in [0, d]$$

r_S is the edge vector function of the rotatory bale and can be written as

$$r_S(t_S, \varphi_S) = \mathbf{R}_T + t_S \cdot \mathbf{e}_{z2}(\varphi_S), t_S \in [0, r_t], \varphi_S \in [0, 2\pi]$$

\mathbf{R}_T is the center position vector of the rotatory bale; r_t is the radius of the table; $\mathbf{e}_{z2}(\varphi_S)$ is the unit circle vector; φ_S is the rotational angles.

(3) The bounds of the sphere point: the fixed sphere point E is attached on the spindle and moves with three linear axes, which locate in the table plane, that is

$$\begin{cases} g_4(\mathbf{x}) = x_{Efmin} - x_{Ef} \leq 0, g_5(\mathbf{x}) = x_{Ef} - x_{Efmax} \leq 0 \\ g_6(\mathbf{x}) = y_{Efmin} - y_{Ef} \leq 0, g_7(\mathbf{x}) = y_{Ef} - y_{Efmax} \leq 0 \\ g_8(\mathbf{x}) = z_{Efmin} - z_{Ef} \leq 0, g_9(\mathbf{x}) = z_{Ef} - z_{Efmax} \leq 0 \\ g_{10}(\mathbf{x}) = \sqrt{x_{Fm}^2 + y_{Fm}^2} - r_t \leq 0 \\ g_{11}(\mathbf{x}) = z_{Fmmin} - z_{Fm} \leq 0, g_{12}(\mathbf{x}) = z_{Fm} - z_{Fmmax} \leq 0 \end{cases} \quad (22)$$

(4) The length of ball bar: the length of ball bar has been made in series with several lengths:

$$g_{13}(\mathbf{x}) = d \in \{d_1, d_2, \dots\} \quad (23)$$

where d_1, d_2, \dots are the dimensional series of the ball bar.

According to the above kinematic synthesis model of RRSS, by substituting the given positions $(x_{omf}^{(i)}, y_{omf}^{(i)}, z_{omf}^{(i)}, \theta_1^{(i)}, \theta_2^{(i)}, i = 1, \dots, n)$ into Equation (19), we can obtain the parameters $(x_{Ef}, y_{Ef}, z_{Ef}, x_{Fm}, y_{Fm}, z_{Fm}, d)$ of RRSS. For installing two balls on the table and the spindle, the parameters of RRSS have to be transformed into the coordinate system of the machine tool, that is

$$\begin{bmatrix} X_{Ef} \\ Y_{Ef} \\ Z_{Ef} \end{bmatrix} = \begin{bmatrix} 0 & 0 & -1 \\ 0 & 1 & 0 \\ 1 & 0 & 0 \end{bmatrix} \cdot \begin{bmatrix} x_{Ef} \\ y_{Ef} \\ z_{Ef} \end{bmatrix} \quad (24)$$

And the installation parameters of RRSS are

$$\left\{ \begin{array}{l} a_2 = \sqrt{x_{Fm}^2 + y_{Fm}^2} \\ s_2 = z_{Fm} \\ \theta_{A0} = \arctan \frac{y_{Fm}}{x_{Fm}} \\ a_0 = \sqrt{x_{E_f}^2 + y_{E_f}^2} \\ s_0 = z_{E_f} \\ \theta_{C0} = \arctan \frac{y_{E_f}}{x_{E_f}} \end{array} \right. \quad (25)$$

As the results of the kinematic synthesis of RRSS are two extreme positions and constraint conditions, we mount the two precision balls at the solved positions, and the DBB test of the two-axis rotary table will cover the full workspace.

4. Actual Parameter Identification of Spatial Five-Bar Linkage for the DBB Test

As previously mentioned, the motion function, range, and dimensions of the spatial RRSS linkage have been determined for the ideal case of the DBB test for a two-axis rotary table. However, the actual dimensions of the RRSS linkage depend on the precise positions of the two balls or the mounting operations on both the table and the spindle, which can cause variations in the RRSS motion. Mounting errors for the two balls can also affect the accuracy of the DBB test. To improve accuracy, it is necessary to identify the installation position errors for the spatial RRSPS linkage.

The spatial five-bar linkage RRSPS for the DBB test of a two-axis rotary table has two degrees of freedom. The angles θ_1 and θ_2 are independently driven by two motors as theoretical input values for the RRSS linkage. In practice, both the two-axis rotary table and the ball positions may have errors, such as geometric errors and elastic deformations. These errors are revealed by the output values of the DBB test, specifically by variations in the length d^* of the RRSPS linkage, as shown in Figure 6.

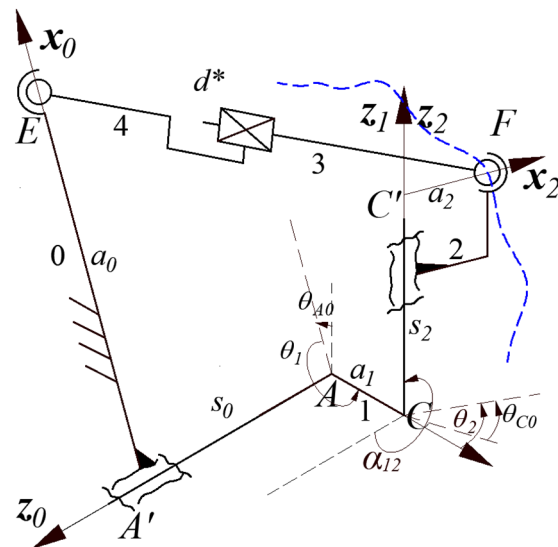


Figure 6. Actual spatial five-bar linkage RRSPS for the DBB test.

According to Equation (8), the RRSPS linkage has eight parameters: six installation position coordinates and two construction parameters. The output value d^* of the DBB test reflects the total error caused by these eight parameters, which can be divided into three types: link parameter errors or installation position errors, construction errors, and kinematic pair errors caused by manufacturing. Kinematic pair errors result in error motion of the moving links with six degrees of freedom [25], but this is a complex topic and is

not discussed in this paper. The first two types of errors can be directly calculated by substituting the actual link lengths into Equation (8) instead of the designated values, which will correspond to the output values d^* of the DBB test.

Conversely, the output data d^* of the DBB test for a two-axis rotary table include the total error caused by eight link parameters and kinematic pair errors. Equation (8) indicates the theoretical relationship between the link parameters and the output value d of the RRSS for the DBB test, providing clues to identify eight-parameter errors from the output data d^* of the DBB test, except for kinematic pair errors. Therefore, we set up a mathematical model, a saddle point programming [24], to identify the actual lengths of the links by letting the maximum error between the measuring values d_i^* and the theoretical calculating values d_i be minimum during a period of DBB test, that is

$$\left\{ \begin{array}{l} \Delta_{MA} = \min_x \max_{1 \leq i \leq n} \{|\delta_{MA}^i(x)|\} = \min_x \max_{1 \leq i \leq n} \left\{ \left| d_i^* - \sqrt{(u_i)^2 + (v_i)^2 + (w_i)^2} \right| \right\} \\ u_i = a_1 \cos \theta_1^i + s_2 \sin \alpha_{12} \sin \theta_1^i + a_2 \cos \theta_1^i \cos \theta_2^i - a_2 \cos \alpha_{12} \sin \theta_1^i \sin \theta_2^i - a_0 \\ v_i = a_1 \sin \theta_1^i - s_2 \sin \alpha_{12} \cos \theta_1^i + a_2 \sin \theta_1^i \cos \theta_2^i + a_2 \cos \alpha_{12} \cos \theta_1^i \sin \theta_2^i \\ w_i = -s_0 + s_2 \cos \alpha_{12} + a_2 \sin \alpha_{12} \sin \theta_2 \\ \theta_1^i = \theta_{1A}^i - \theta_{A0} - 90^\circ \\ \theta_2^i = \theta_{2C}^i + \theta_{C0} \\ s.t. \quad a_0, a_1, a_2, s_0, s_2 \in (-\infty, +\infty) \\ \alpha_{12} \in [0, 2\pi) \quad \theta_{A0}, \theta_{C0} \in [-\pi, \pi) \\ x = (a_0, a_1, a_2, s_0, s_2, \alpha_{12}, \theta_{A0}, \theta_{C0})^T \end{array} \right. \quad (26)$$

where the objective function $\{\delta_{MA}^i(x)\}$ is the corresponding error between the measured value d_i^* of the DBB test and the calculated output value d_i of the RR-SPS linkage for all instances $i = 1, 2, \dots, n$, the optimization variables $x = (s_0, a_0, \theta_{A0}, s_2, a_2, \theta_{C0}, a_1, \alpha_{12})^T$ are the eight parameters of RR-SPS linkage, respectively; n is the number of discrete points $\{d_i^*\}$ measured by the DBB test, and Δ_{MA} is the saddle optimization error for $\{d_i^*\}$, which is the unidentified errors caused by manufacturing, such as the kinematic pairs errors.

After obtaining the measured data d^* , it is incorporated into the identification model as per Equation (26). The design values of the mechanism are used as initial values for this computation. This process allows for the calculation of the actual dimensions $(s_0, a_0, \theta_{A0}, s_2, a_2, \theta_{C0}, a_1, \alpha_{12})$ of the mechanism. Subsequently, we can determine the installation error of the ball bar and the structural error of the machine tool under testing.

5. Experiments of the Double Ball Bar Test of the Two-Axis Rotary Table

The new saddle synthesis models for the spatial linkages of a two-axis rotary table, as presented in the previous sections, are designed to measure the motion function and range and identify the actual dimension parameters. These models can be verified through several experiments, in which data from the DBB tests are measured in various cases. The results demonstrate that this approach is effective in improving the accuracy of DBB tests for machine tools.

A five-axis vertical machining center with an A and C two-axis rotary table is used as the test subject for these experiments. The spindle has a linear feed motion in the X, Y, and Z directions. The structure of the machine tool is shown in Figure 7, and its main technical parameters are listed in Table 1.

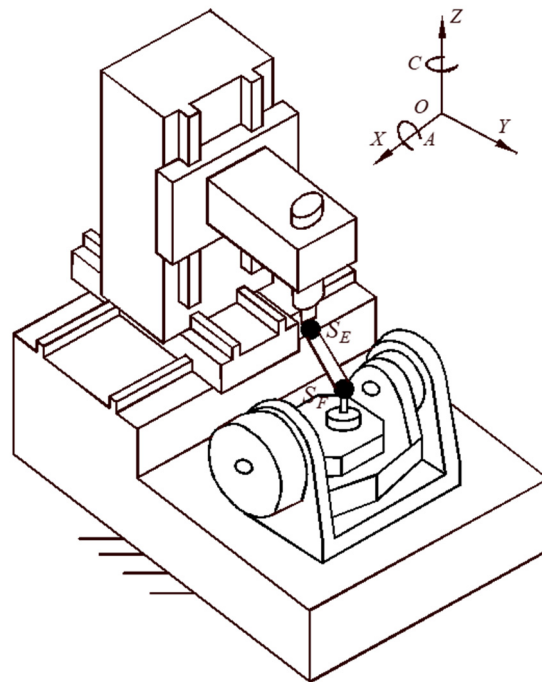


Figure 7. The five-axis vertical machining center.

Table 1. Design constructure parameters of five-axis vertical machining center.

Technical Parameters	Value	Unit
X/Y/Z travel	650/650/450	mm
A-axis motion range	$-130^{\circ}\sim+130^{\circ}$	$^{\circ}$
C-axis motion range	$0\sim360$	$^{\circ}$
Table diameter	$\Phi 650$	mm
Distance from spindle end face to table	90~540	mm
Perpendicular distance of AC axis line (a_1)	0	mm
Included angle of AC axis line (α_{12})	270	$^{\circ}$

The Renishaw QC-20W is chosen as the DBB for testing, whose measuring range is ± 1 mm. The five-axis vertical machining center has a compensation range for the A-axis with $-110^{\circ}\sim+110^{\circ}$, despite its original motion range within $-130^{\circ}\sim+130^{\circ}$.

Based on the kinematic synthesis models of linkages mentioned above, the measurement motion function and ranges can be designed, and the actual dimension parameters need to be identified for the DBB test of the two-axis rotary table, respectively, which are verified by the several experiments designed as follows.

5.1. Measurement Motion Function and Range of the DBB Test

The first experiment is designed to verify the measurement motion function and motion range, which are critical aspects of the spatial linkages of a two-axis rotary table. The experiment is conducted with known conditions, assigned tasks, and requirements, as described below.

Known conditions: The design construction parameters ($a_1 = 0$, $\alpha_{12} = 270^{\circ}$) of the A and C two-axis rotary table are known. The rotational angle θ_1 of the A-axis has bounds of $\pm 110^{\circ}$, and the rotational angle θ_2 of the C-axis has bounds of 360° , as shown in Table 1.

Assigned tasks: The measurement motion function and motion range are calculated and verified by DBB tests of the two-axis rotary table of a five-axis vertical machining center, based on the saddle synthesis models of spatial linkages established in this paper.

Requirements: The installation of two balls for the DBB test must be performed only once to cover the entire motion range of the two-axis rotary table efficiently. Interference

between the rod of the DBB and the rotary table must be avoided when the A-axis moves within $\pm 110^\circ$. This means that link 2 rotates its angle θ_1 ($0\text{--}360^\circ$) while link 0 has values θ_1 ($-110^\circ, 110^\circ$).

All these parameters, conditions, and requirements are incorporated into the objective or subjective functions of the saddle synthesis models for spatial linkages of the two-axis rotary table. By substituting them into Equations (18) and (19), along with the initial values for optimization variables, subject function constraints, and bounds for optimization variables, we can solve optimization Equations (18) and (19). The results provide us with installation positions ($s_0, a_0, \theta_{A0}, s_2, a_2, \theta_{C0}$) for the two precision balls of the RRSS linkage, as shown in Table 2, and the length d of the DBB is determined to be a nominal length of $d = 300$ mm.

Table 2. The parameters of synthesized RRSS linkage.

	s_0/mm	a_0/mm	$\theta_{A0}/^\circ$	s_2/mm	a_2/mm	$\theta_{C0}/^\circ$
angle measurement range as $-110^\circ\sim 0^\circ$	96.310	352.114	-55.000	80.000	30.000	-161.592
angle measurement range as $0^\circ\sim +110^\circ$	96.310	352.114	55.000	80.000	30.000	-161.592

According to the parameters ($s_0, a_0, \theta_{A0}, s_2, a_2, \theta_{C0}$) of the synthesized RRSS linkage in Table 2, we precisely locate the positions of two balls on the spindle and the worktable, respectively. And θ_2 ($0, 360^\circ$) is the independent variable, and θ_1 ($-110^\circ, 110^\circ$) is the dependent variable calculated by Equation (10).

By incorporating the functional relationship between the mechanism size and θ_1 and θ_2 into Equation (7), we can determine the position of the fixed ball point E of the DBB and the spatial trajectory formed by the moving ball point F in the fixed coordinate system, as shown in Figure 8. The blue grid represents a spherical surface with E as the center and the nominal length d of the DBB as the radius. The trajectory of F is a spatial curve on this spherical surface. The red line represents the line connecting the moving ball points and the fixed ball point of the DBB at each moment in time.

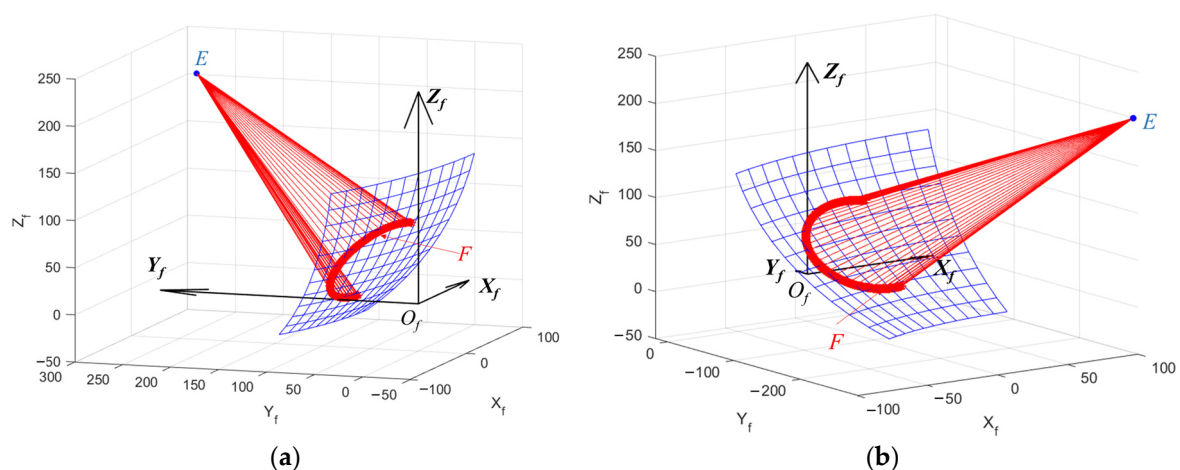


Figure 8. Calculation trajectory of the moving ball point and the fixed ball point; (a) angle measurement range as $-110^\circ\sim 0^\circ$; (b) angle measurement range as $0^\circ\sim +110^\circ$.

The motion ranges of the two-axis rotary table are measured by the DBB test, shown in Figure 9, which is the same as that of the synthesized RRSS linkage.

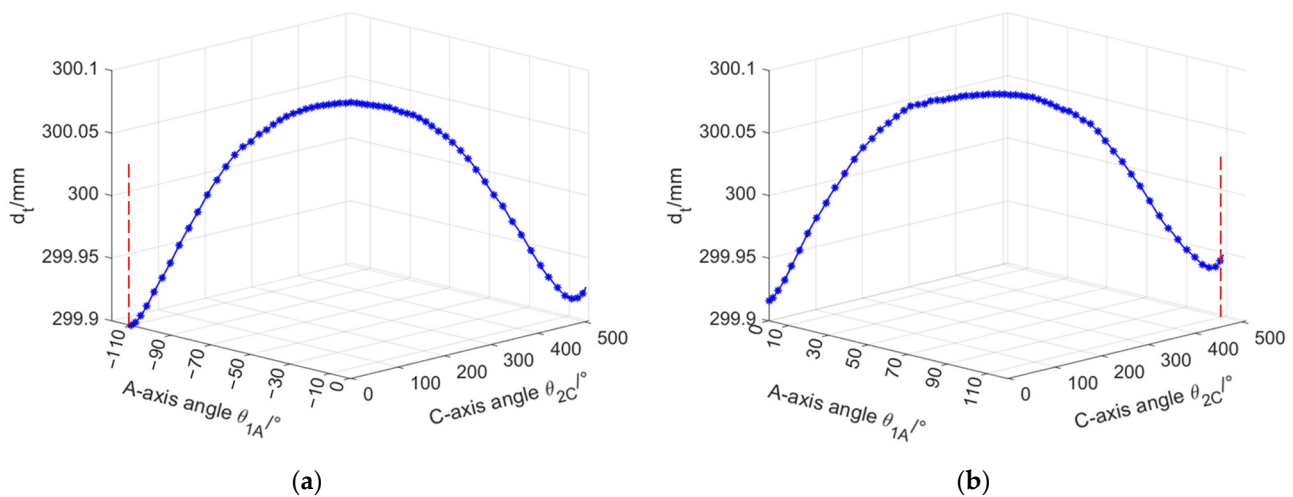


Figure 9. The workspace of two-axis A and C calculated; (a) angle measurement range as $-110^{\circ}\sim 0^{\circ}$; (b) angle measurement range as $0^{\circ}\sim +110^{\circ}$.

From the data presented in Table 2 and Figures 8 and 9, it is clear that the measurement motion function and motion range of the two-axis rotary table DBB test have successfully met the tasks, conditions, and requirements for the experiments with the A and C two-axis rotary table. The measuring data indicate that the DBB test runs continuously within the range of the C-axis θ_2 ($0\sim 360^{\circ}$) and the range of the A-axis θ_1 ($-110^{\circ}, 110^{\circ}$). These results provide evidence that the novel optimization synthesis model of RRSS proposed in this paper is perfectly suitable for designing the measurement motion of DBB tests for a two-axis rotary table.

5.2. The Actual Parameter Identification of the DBB Test

This experiment, which was designed to verify the parameter identification of the two-axis rotary table DBB test, is conducted under known conditions and specific tasks. It is structured around three cases and four steps. The design parameters of the A and C two-axis rotary table are given, and the mounting position coordinates of two precision balls are listed. The task is to identify the actual parameters of the RRSS linkage corresponding to the DBB test of the two-axis rotary table. Three cases of DBB tests are designed, and each case involves specific adjustments to the parameters or conditions, which are described as follows:

Known conditions: The design parameters ($a_1 = 0, \alpha_{12} = 270^{\circ}, \theta_1 = -110\sim 110^{\circ}, \theta_2 = 0\sim 360^{\circ}$) of the A and C two-axis rotary table are given in Table 1. The mounting position coordinates ($s_0, a_0, \theta_{A0}, s_2, a_2, \theta_{C0}$) of two precision balls are listed in Table 2.

Assigned tasks: The task is to identify the actual parameters of the RRSS linkage corresponding to the DBB test of the two-axis rotary table.

Experiment cases: Three cases of DBB tests are designed as M1 to M3, shown in Figure 10.

Case M1: The mounting positions coordinates ($s_0, a_0, \theta_{A0}, s_2, a_2, \theta_{C0}$) of two balls are located as per Table 2.

Case M2: The parameter $s_0^{(2)}$ is assigned to be $s_0 + 0.2$ mm. This is achieved by operating the linear axis-X by CNC, while other linear axes maintain the same fixed values as in case M1.

Case M3: The parameter $s_0^{(3)}$ is designated to be $s_0 - 0.2$ mm. This is also achieved by operating the linear axis-X by CNC, with other linear axes maintaining the same fixed values as in case M1.

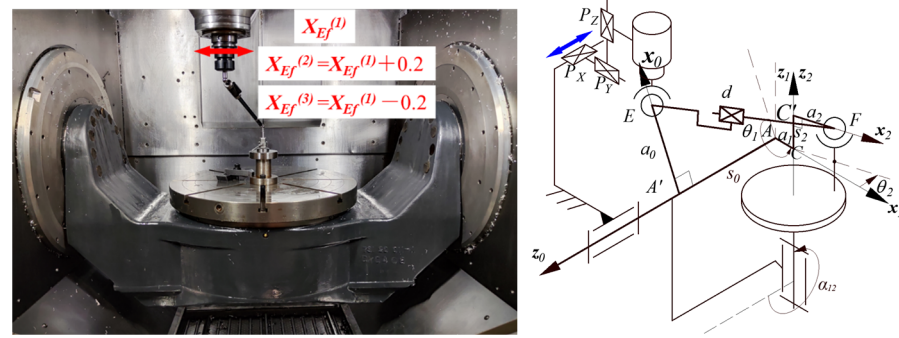


Figure 10. The DBB test of two-axis rotary table in three cases.

The experiment is conducted in four steps to verify the parameter identification of the two-axis rotary table DBB test:

Step 1: Utilizing the six parameters ($s_0, a_0, \theta_{A0}, s_2, a_2, \theta_{C0}$) of the spatial five-bar linkage RRRSPS synthesized in Table 2, the installation positions of the moving and fixed ball points are calculated. The machine tool spindle's X, Y, and Z linear axes are controlled to install the ball seat at the corresponding positions. The fixed ball point is installed on the spindle, and the moving ball point is installed on the worktable. The machine tool is controlled to move according to the parameters designed by Formulas (10) and (11), realizing the DBB test of the two-axis turntable. All these d_1^* values are taken as the data for case M1, shown as an orange * line in Figure 11.

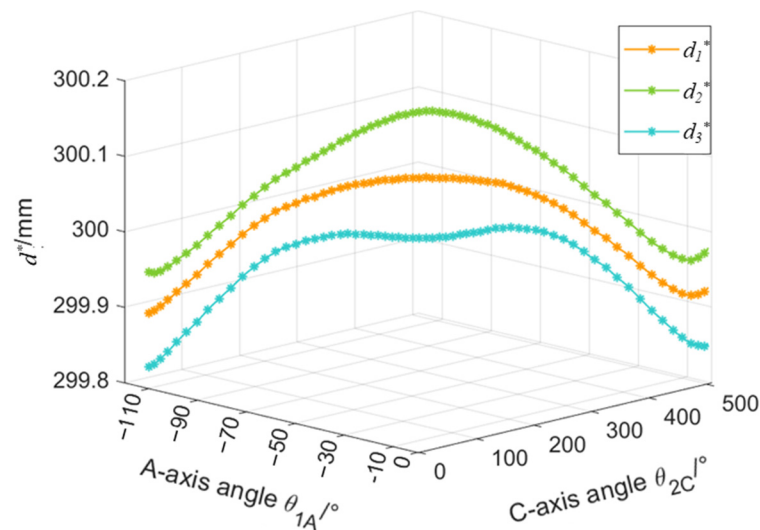


Figure 11. The data of DBB test in three cases.

Step 2: The parameter $s_0^{(2)}$ is adjusted to $s_0 + 0.2$ mm. This means that while the position of the moving ball point relative to the machine tool worktable remains unchanged, only $X_{Ef}^{(2)}$ of the fixed ball point's three linear axes moves 0.2 mm in the negative direction relative to $X_{Ef}^{(1)}$. The DBB test of the two-axis rotary table is synchronously measured, and the output data d_2^* of the DBB test is recorded as the data for case M2, shown as a green line in Figure 11.

Step 3: The parameter $s_0^{(3)}$ is adjusted to $s_0 - 0.2$ mm. This means that while the position of the moving ball point relative to the machine tool worktable remains unchanged, only $X_{Ef}^{(3)}$ of the fixed ball point's three linear axes moves 0.2 mm in the positive direction relative to $X_{Ef}^{(1)}$. The DBB test of the two-axis rotary table is synchronously measured, and the output data d_3^* of the DBB test is taken as data for case M3, shown as a blue dashed line in Figure 11.

Step 4: The data $\{d_1^*\}$, $\{d_2^*\}$, and $\{d_3^*\}$ from all three cases are substituted into mathematical model (26). These equations are solved with identical initial values for the optimization variables to obtain identification results. The actual eight parameters ($s_0, a_0, \theta_{A0}, s_2, a_2, \theta_{C0}, a_1, \alpha_{12}$) of the five-bar linkage RRSPS for all three cases are completely identified by Equation (26) based on measured data case M1-M3 and are listed in Table 3.

Table 3. Parameters of RRSPS linkage identified in three cases.

	s_0/mm	a_0/mm	$\theta_{A0}/^\circ$	s_2/mm	a_2/mm	$\theta_{C0}/^\circ$	a_1/mm	$\alpha_{12}/^\circ$
Case M1	96.865	351.891	-54.995	79.871	30.063	-161.531	-0.023	270.093
Case M2	97.124	351.900	-54.996	79.904	30.080	-161.541	-0.021	270.102
Case M3	96.682	351.951	-54.996	79.934	30.111	-161.559	-0.019	270.094
Design value	96.310	352.114	-55.000	80.000	30.000	-161.592	0	270.000

In the identification results listed in Table 3, it is only the parameter s_0 that shows a significant difference across the three cases, that is

$$\begin{cases} s_0^{(2)} - s_0^{(1)} = 97.124 - 96.865 = 0.259 \\ s_0^{(3)} - s_0^{(1)} = 96.682 - 96.865 = -0.183 \end{cases} \quad (27)$$

According to the results in Equation (27), the parameters assigned in the three cases are correctly identified. The values are close to the assigned values of $s_0, s_0 - 0.2 s_0 + 0.2$. The other seven parameters ($a_0, \theta_{A0}, s_2, a_2, \theta_{C0}, a_1, \alpha_{12}$) show only slight variations. This suggests that the identification process is accurate and reliable for these parameters.

By substituting the mechanism size parameters ($s_0, a_0, \theta_{A0}, s_2, a_2, \theta_{C0}, a_1, \alpha_{12}$) identified in Table 3 and the mechanism input angle parameters θ_1 and θ_2 into Equation (8), we can calculate the output d of the mechanism under the identified parameters, which is the ideal length of the DBB. A comparison of this calculated output with actual test results provides valuable insights into the accuracy of our parameter identification process and the effectiveness of our computational model. As shown in Figure 12, test results are represented by colored * marks, while the corresponding mechanism output is depicted as a black solid line.

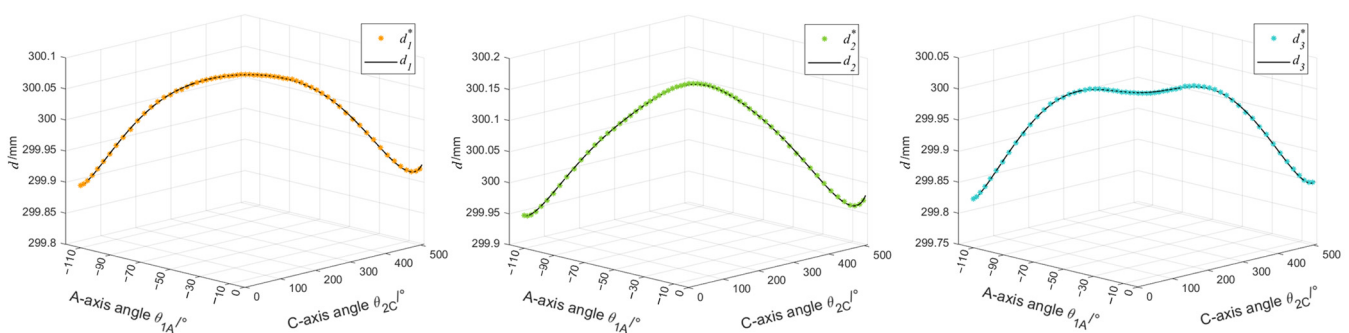


Figure 12. Comparison of test results and mechanism output under identification parameters.

We can calculate the maximum deviation between the DBB measurements and the mechanism output under the identified parameters during the three case measurement processes, which is represented as Δ_{MA} in the identification model (26). Its values are shown in Table 4.

Table 4. Calculated values of Δ_{MA} in three cases.

	Case M1	Case M2	Case M3
$\Delta_{MA}/\mu\text{m}$	1.587	1.607	1.674

As per Figure 12 and Table 4, the curves representing the test data and the calculated data in the three cases are closely aligned. The maximum deviations between the two sets of data are also very similar. This indicates that our parameter identification method is reliable and our computational model is robust.

The aforementioned experiments validate the accuracy and effectiveness of the real parameter identification model for the RRSPS five-bar mechanism through three case studies. This provides a reliable methodology for enhancing the testing precision of the two-axis rotary table DBB in machine tools. Furthermore, it establishes a foundation for exploring specific applications such as compensation for two-axis rotary tables in machine tools.

6. Conclusions

Based on the theoretical derivations and experimental measurements conducted for the DBB test of the two-axis rotary table of machine tools, we can draw the following conclusions:

(1) The novel synthesis model of the spatial four-bar linkage RRSS, as presented in this paper, provides an effective method for designing the measurement motion function and motion range of the DBB test for the two-axis rotary table of machine tools.

(2) The newly proposed kinematic synthesis model of the spatial five-bar linkage RRSPS is a precise and effective method for identifying the actual parameters in the DBB test of the two-axis rotary table. This provides a reliable methodology for improving the test accuracy of the DBB test for the two-axis rotary table of machine tools.

(3) The kinematic analysis and synthesis of spatial linkages offer a new theoretical basis for the DBB test of the two-axis rotary table of machine tools, and it is a new application field in this area.

Author Contributions: Conceptualization, Z.L. and D.W.; methodology, Z.L. and S.T.; software, S.T.; validation, Z.L.; data curation, S.T.; writing—original draft preparation, Z.L. and S.T.; writing—review and editing, D.W.; project administration, Z.L.; All authors have read and agreed to the published version of the manuscript.

Funding: This research received no external funding.

Data Availability Statement: The original data contributions presented in the study are included in the article; further inquiries can be directed to the corresponding authors.

Conflicts of Interest: The authors declare no conflict of interest.

References

1. Hunt, K.H. *Kinematic Geometry of Mechanisms*; Oxford University Press: Oxford, UK, 1978.
2. McCarthy, J.M.; Soh, C.S. *Geometric Design of Linkages*, 2nd ed.; Interdisciplinary Applied Mathematics 11; Springer: New York, NY, USA, 2010.
3. Bryan, J. A simple method for testing measuring machines and machine tools Part 1: Principles and applications. *Precis. Eng.* **1982**, *4*, 61–69. [[CrossRef](#)]
4. Bryan, J. A simple method for testing measuring machines and machine tools Part 2: Construction details. *Precis. Eng.* **1982**, *4*, 125–138. [[CrossRef](#)]
5. *ISO 230-4; Test Code for Machine Tools-Part 4: Circular Tests for Numerically Controlled Machine Tools*. ISO: London, UK, 2005.
6. *ASME B5.54; Methods for Performance Evaluation of Computer Numerically Controlled Machining Centers*. American National Standards Institute: Washington, DC, USA, 2005.
7. Huang, Y.B.; Fan, K.C.; Lou, Z.F.; Sun, W. A Novel Modeling of Volumetric Errors of Three-Axis Machine Tools Based on Abbe and Bryan Principles. *Int. J. Mach. Tools Manuf.* **2020**, *151*, 103527. [[CrossRef](#)]
8. Lee, K.I.; Yang, S.H. Accuracy Evaluation of Machine Tools by Modeling Spherical Deviation Based on Double Ball-Bar Measurements. *Int. J. Mach. Tools Manuf.* **2013**, *75*, 46–54. [[CrossRef](#)]
9. Lei, W.T.; Sung, M.P.; Liu, W.L. Double Ballbar Test for the Rotary Axes of Five-Axis CNC Machine Tools. *Int. J. Mach. Tools Manuf.* **2007**, *47*, 273–285. [[CrossRef](#)]
10. Lasemi, A.; Xue, D.; Gu, P. Accurate Identification and Compensation of Geometric Errors of 5-Axis CNC Machine Tools Using Double Ball Bar. *Meas. Sci. Technol.* **2016**, *27*, 055004. [[CrossRef](#)]

11. Chen, J.; Lin, S.; He, B. Geometric Error Measurement and Identification for Rotary Table of Multi-Axis Machine Tool Using Double Ballbar. *Int. J. Mach. Tools Manuf.* **2014**, *77*, 47–55. [[CrossRef](#)]
12. Zhu, S.; Ding, G.; Qin, S. Integrated Geometric Error Modeling, Identification and Compensation of CNC Machine Tools. *Int. J. Mach. Tools Manuf.* **2012**, *52*, 24–29. [[CrossRef](#)]
13. Pahk, H.J.; Kim, Y.S.; Moon, J.H. A new technique for volumetric error assessment of CNC machine tools incorporating ball bar measurement and 3D volumetric error model. *Int. J. Mach. Tools Manuf.* **1997**, *37*, 1583–1596. [[CrossRef](#)]
14. Zhong, L.; Bi, Q.; Wang, Y. Volumetric accuracy evaluation for five-axis machine tools by modeling spherical deviation based on double ball-bar kinematic test. *Int. J. Mach. Tools Manuf.* **2017**, *122*, 106–119. [[CrossRef](#)]
15. Xu, K.; Li, G.; He, K.; Tao, X. Identification of Position-Dependent Geometric Errors with Non-Integer Exponents for Linear Axis Using Double Ball Bar. *Int. J. Mech. Sci.* **2020**, *170*, 105326. [[CrossRef](#)]
16. Xia, C.; Wang, S.; Wang, S.; Ma, C.; Xu, K. Geometric error identification and compensation for rotary worktable of gear profile grinding machines based on single-axis motion measurement and actual inverse kinematic model. *Mech. Mach. Theor.* **2021**, *155*, 104042. [[CrossRef](#)]
17. Xia, H.-J.; Peng, W.-C.; Ouyang, X.-B.; Chen, X.-D.; Wang, S.-J. Identification of geometric errors of rotary axis on multi-axis machine tool based on kinematic analysis method using double ball bar. *Int. J. Mach. Tools Manuf.* **2017**, *122*, 161–175. [[CrossRef](#)]
18. Chai, X.; Zhang, N.; He, L.; Li, Q.; Ye, W. Kinematic Sensitivity Analysis and Dimensional Synthesis of a Redundantly Actuated Parallel Robot for Friction Stir Welding. *Chin. J. Mech. Eng.* **2020**, *33*, 1–10. [[CrossRef](#)]
19. Bai, S.; Li, Z.; Angeles, J. Exact Path Synthesis of RCCC Linkages for a Maximum of Nine Prescribed Positions. *ASME J. Mech. Robot.* **2022**, *14*, 021011. [[CrossRef](#)]
20. Chen, C.; Angeles, J. A novel family of linkages for advanced motion synthesis. *Mech. Mach. Theory* **2008**, *43*, 882–890. [[CrossRef](#)]
21. Zhao, C.; Guo, W. Inverted Modelling: An Effective Way to Support Motion Planning of Legged Mobile Robots. *Chin. J. Mech. Eng.* **2023**, *36*, 19. [[CrossRef](#)]
22. Huang, X.; Liu, C.; Xu, H.; Li, Q. Displacement Analysis of Spatial Linkage Mechanisms Based on Conformal Geometric Algebra. *J. Mech. Eng.* **2021**, *57*, 39–50.
23. Denavit, J.; Hartenberg, R.S. A Kinematic Notation for Lower-Pair Mechanisms Based on Matrices. *J. Appl. Mech.* **1955**, *22*, 215–221. [[CrossRef](#)]
24. Wang, D.; Wang, W. *Kinematic Differential Geometry and Saddle Synthesis of Linkages*; John Wiley & Sons: Singapore, 2015.
25. Wang, D.; Wang, Z.; Wu, Y.; Dong, H.; Yu, S. Invariant errors of discrete motion constrained by actual kinematic pairs. *Mech. Mach. Theory* **2018**, *119*, 74–90. [[CrossRef](#)]

Disclaimer/Publisher’s Note: The statements, opinions and data contained in all publications are solely those of the individual author(s) and contributor(s) and not of MDPI and/or the editor(s). MDPI and/or the editor(s) disclaim responsibility for any injury to people or property resulting from any ideas, methods, instructions or products referred to in the content.